Polymers from Renewable Sources. IV. Polyurethane Elastomers Based on Myrcene Polyols

J. L. CAWSE,* J. L. STANFORD, and R. H. STILL, *Wolfson Polymer Research Unit, Department of Polymer Science and Technology, University of Manchester Institute of Science and Technology, P. O. Box 88, Manchester, M60 1QD, United Kingdom*

Synopsis

Two hydroxy-functionalized liquid rubbers, one a commercially available polybutadiene (PB) and the other a specially synthesized polymyrcene (PM), have been converted into homopolyurethane elastomers by reaction with 4,4'-diphenylmethane diisocyanate (MDI). Additionally, PB and PM, each in admixture with various amounts of 1,4-butane diol, were reacted with MDI to yield two series of segmented copolyurethanes having different hard-block contents (0–30% w/w). The physical properties of these elastomers have been compared by stress–strain, thermal, and dynamic mechanical analyses, and by swelling experiments. The two series of segmented copolyurethanes have similar morphologies being almost completely phase-separated and variations in physical properties have been empirically related to hard block contents. The PM-based elastomers exhibited higher T_g values, ultimate elongations, and larger swelling ratios, but were softer and possessed lower tensile strengths in comparison with elastomers based on PB. These differences have been related to solfraction contents, the nature and distribution of molecular species present in the parent liquid rubbers and hence to polyol functionalities ($\bar{f}_n$). Analysis of the stress–strain data from the homopolyurethanes using the Mooney–Rivlin expression enabled the relationship between $\bar{f}_n$ and elastomer structure to be quantified in terms of the molar mass ($\bar{M}_c$) of the polyurethane network chains forming the soft blocks.

INTRODUCTION

Polyurethanes (PUs) derived from hydroxy functionalized polybutadienes (PBs) have found use in solid rocket motors[1,2] and as adhesives,[3] sealants,[4] and potting compounds.[5] These applications arise, in part, from the low water uptake of these PUs and their ability to be molded *in situ* from liquid components. PBs are generally obtained from butadiene by free radical[6,7] or anionically[8] initiated polymerization.

PBs on reaction with diisocyanates yield elastomers whose tensile and tear strengths are low compared to PU elastomers derived from polyether- and polyester-based polyols.[9] However, some improvement in properties may be achieved for PB-based elastomers by the incorporation of a low molecular weight diol or diamine as a chain extender into the PU-forming reaction mixture. This generates a copolyurethane with a domain-type morphology comprising a two-phase structure with crystalline, chain-extended

* Present address: Ilford Ltd., Mobberley, Knutsford, Cheshire, WA16 7H7, United Kingdom.

Journal of Applied Polymer Science, Vol. 31, 1549–1565 (1986)
 CCC 0021-8995/86/061549-17$04.00

units embedded in a rubbery PB-based matrix. These two phases, the "hard" and "soft" segments, respectively, are chemically different, and demixing occurs by virtue of thermodynamic incompatibility.[10]

This paper reports a study of structure–property relations of similar copolyurethanes formed by reactions involving a novel myrcene polyol (PM),[11] in admixture with 1,4-butane diol (BD) and 4.4′-diphenylmethane diisocyanate (MDI). The properties of the copolyurethanes so formed have been compared with similar polymers derived from PB/BD mixtures on reaction with MDI. Hard segment contents were varied between 0 and 30% by weight to optimize physical properties.

EXPERIMENTAL

Materials

The polymyrcene (PM) polyol was prepared as described in a previous paper[11] using myrcene (200 mL), *n*-butanol (133 mL), and 50% aqueous hydrogen peroxide (20 mL). The PB polyol used was a hydroxy-functionalized, butadiene homopolymer, Arco R45-HT (Cornelius Chemical Co.). Both polyols were purified and analyzed using acetylation, GPC, and VPO techniques described previously.[11] The characterization data obtained for PB and PM polyols are presented in Table I. Additional characterization of the PM polyol by NMR gave the following structural composition: 1,4 units, 77%; 1,2 units, ~0%; 3,4 units, 23%. The composition of the PB polyol was evaluated using the IR method of Brunette et al.,[12] as 1,4 content, 60% (trans) and 5% (cis); 1,2 content, 35%. The chain extender, 1,4-butane diol (BD), was distilled *in vacuo* before use and 4,4′-diphenylmethane diisocyanate (MDI) (Bayer flake) was melted and filtered before use. It had a purity of >99% as assessed by titrimetry.[13]

Polymer Preparation

Polymers prepared from PM and PB polyols are listed in Table II. The segmented copolyurethanes were prepared by a prepolymer technique similar to that described by Schneider and Matton.[14] A 4% excess of isocyanate groups over the required for stoichiometric equivalence of hydroxyl and isocyanate groupings was used. Molar ratios were calculated using the

TABLE I
Molar Mass, Equivalent Weight ($\bar{E}_n$), and Functionality Data of PB and PM Polyols

Polyol	$\bar{E}_n$[a]	$\bar{M}_n$ (GPC)[b]	$\bar{M}_w$ (GPC)	$\bar{M}_w/\bar{M}_n$ (GPC)	$\bar{f}_n$[c]	$\bar{M}_n$ (VPO)[d]	$\bar{f}_n$[e]
PM	1322	2950	4100	1.39	2.23	2110	1.60
PB	1088	2919	4965	1.70	2.68	2343	2.15

[a] $\bar{E}_n$ is defined as the molar mass per hydroxyl group present in the polyols or products extracted from them.
[b] GPC[11]; tetrahydrofuran, 23°C, PPO calibration.
[c] $\bar{F}_n = \bar{M}_n/\bar{E}_n$; $\bar{M}_n$ from GPC data.
[d] VPO[11]; toluene 60°C, benzil calibration.
[e] $\bar{f}_n$; $\bar{M}_n$ from VPO data.

TABLE II
Copolyurethanes: Preparation and Properties

Polymer[a] code	Weight ratio MDI:LR[b] :BD	% hard block[c]	Appearance of elastomer	Density ($10^3 \times$ kg m^{-3})
PMO	1.00:10.04:0.00	0	Colorless, transparent, soft	0.952
PM10	1.00: 5.16:0.17	10.0	White,soft	0.981
PM20	1.00: 3.24:0.22	18.3	White,soft	1.005
PM30	1.00: 2.09:0.26	29.4	White,tough	1.037
PB0	1.00: 8.28:0.00	0	Colorless, resilient, transparent	0.942
PB10	1.00: 4.82:0.16	10.1	White,tough	0.966
PB20	1.00: 2.96:0.22	19.7	White,tough	1.002
PB30	1.00: 2.04:0.26	29.9	Cream,tough	1.029

[a] PM = polymyrcene, PB = polybutadiene; numbers are nominal hard block contents.
[b] LR = liquid rubber (PM or PB).
[c] Defined as wt of BD + wt of MDI stoichiometrically equivalent to BD as a percentage of total wt of reactants (BD + MDI + LR).

equivalent weights of the respective polyols obtained by acetylation. For the PM series of polymers, MDI and the liquid polyol were reacted under vacuum at 70°C, with continuous stirring for 1 h. BD was then added to the cloudy prepolymer and stirring continued *in vacuo* until the reaction mixture clarified (~1 min), when it was poured into a flat, PTFE mold and cured at 105°C for 2 h followed by 14 h at 80°C.

For the PB-based series of copolyurethanes, the prepolymer stage had to be modified for those materials containing 10% w/w hard block or less. A prepolymer reaction time of 10 min was employed since gelation occurred[15] if longer reaction times were used. The procedure adopted for curing and for the preparation of the PB-based elastomers was as described for the PM systems. Copolymers in both elastomer series with hard block contents greater than 30% w/w were of a "cheesy" consistency, possessed negligible physical strength, and therefore were not studied in detail. Samples were stored for at least a weak over silica gel before testing.

POLYMER CHARACTERIZATION

(a) Stress–Strain Measurements were carried out at 18°C at an extension speed of 20 mm min^{-1} on dumbbell specimens of 40 mm gauge length, 4 mm width, and 2.5 mm thickness using an Instron Model 1122 Universal Tensile Tester.

(b) Dynamic Mechanical Spectra were obtained form G'/T and trans δ/T data recorded using a torsion pendulum at an operating frequency of $\simeq$ 1 Hz over the temperature range −180 to + 200°C as previously described.[16]

(c) Differential Scanning Calorimetry (DSC) was carried out on a DuPont 990 Thermal Analyser with a DSC attachment. Samples (10–15 mg) and glass beads (10 mg) as inert reference material were sealed in aluminium pans and cooled from ambient to −150°C in the apparatus and

then heated at 20°C min^{-1} to 200°C. Glass transition and heat capacity measurements were made as previously reported.[16]

(d) Equilibrium Swelling Ratios and Sol Fractions were measured by immersing rectangular (2.5 × 20 mm) samples in toluene at 20°C for 48 h. The toluene was decanted and removed by rotary film evaporation to yield the soluble material. Volume swelling ratios were evaluated from pre- and post-swelling dimensions.

(e) Water Uptake Studies were made at 20°C on rectangular specimens (2.5 × 20 × 20 mm) immersed in water until the equilibrium uptake of water was achieved as shown by weighting (~10 days).

RESULTS AND DISCUSSION

Structures of the PU Elastomers

The technique of end-capping a high molecular weight polyol with diisocyanate followed by the addition of a low molecular weight "chain extender" tends to favor the formation and development of a highly phase segregated structure in conventional polyurethanes (PUs).[9] The materials which can be produced have vastly different properties which arise essentially form the different proportions of the two structural units present, namely, the hard and soft segments. These segments are formed respectively by reactions of the chain extender with the diisocyanate and the polyol with the diisocyanate. The phase-separated structure in PU elastomers comprises a continuous soft block matrix containing dispersed hard blocks which behave as pseudocrosslinks and filler particles. When the concentration of hard blocks exceeds 50% w/w, they coalesce during PU formation, resulting in phase inversion. This behavior leads to a high-modulus matrix with a dispersed soft segment phase. MDI-based copolyurethanes are known to possess both types of morphology,[17] and similar phase-separated structures were recently reported for copolyurethanes derived from furan-based diisocyanates.[16]

The copolymers prepared in this study contain the hard segment structural units (A) and the idealized soft segment units (B) shown below:

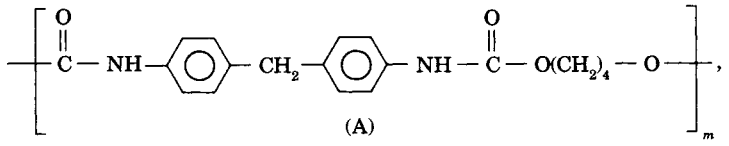

(A)

$m = 1\text{–}5$

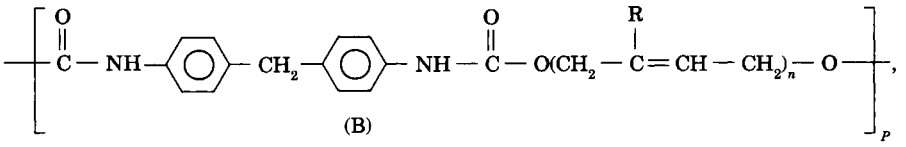

(B)

$P = 1,2,\cdots$

In the soft segments (B), R in the PB polyol moiety is H, and $\bar{n} \approx 55$ from $\bar{M}_n$ (GPC), while R in the PM polyol moiety is $-C_6H_{11}$ and $\bar{n} \approx 22$ from $\bar{M}_n$ (GPC). The PM and PB units shown in (B) are the most dominant of

all the microstructural units present in the original polyols, namely, the trans isomer formed by 1,4 propagation. The other structrual units present and the detailed analysis of the microstructures of the PB and PM chains are reported in detail in the previous paper.[11] The two series of homo- and copolymers thus show different physical properties which are governed by the different soft-block structures present. In addition, the polymers differ in the amounts of sol fraction present and in the degrees of crosslinking which are related to the different functionalities of the liquid rubber precursors from which the PUs were derived.

Thermal Analysis Studies

Differential Scanning Calorimetry (DSC)

DSC studies [Fig. 1(a)] indicate that two main transitions are seen for both series of copolymers. These are a glass transition associated with the soft segment, $T_g{}^S$, and melting behaviour associated with the hard segment, T_m, $T_g{}^S$ is clearly visible in all the systems studied, but the T_m is only prominent in systems having 20 or 30% w/w hard block content. The glass transition $T_g{}^H$, associated with amorphous regions in the hard block segments, cannot be detected even at maximum sensitivity on cured samples unless these have been quench-cooled from above the T_m. In quench cooled systems, $T_g{}^H$ varies between 60 and 80°C, and there is a premelt exotherm between 100 and 140°C [Fig. 1(b)]. Efficient phase separation appears to have occurred in the curd systems, a conclusion based on three main observations: (a) The location of $T_g{}^S$ remains essentially constant irrespective of hard block content and at a value similar to those observed for PM0 and PB0. (b) These T_g values are also very close to those observed for the parent polyols, namely, −57°C for the PM polyol and −81°C for Arco R45-HT. (c) The heat capacity change, ΔC_p, observed at $T_g{}^S$ and normalized for sample mass (m), decreases as a linear function of hard block content,[17] as shown in Figure 2. The experimental values obtained for $\Delta C_p/m$ thus fall on the lines joining the measured value for the matrices PM0 or PB0 with zero, which is the value expected for systems containing no liquid rubber. This indicates that the soft segments contribute to the heat capacity change in direct proportion to their nominal weight fractions. These observations are in accord with the behavior expected from a simple two-phase system in which there is no interphase interaction. Such behavior is to be expected from a consideration of the differences in chemical and physical nature of the hydrocarbon rubber and the polar, extensively hydrogen-bonded hard block segments.

Dynamic Mechanical Analysis (DMA)

Results from DMA confirm and supplement the data provided by DSC. DMA curves [Fig. 3 (a–c)] show that both PM- and PB-based PUs behave in a similar manner, differing only in detail. Thus, both series show a low temperature β-relaxation, as well as an α-relaxation which is asociated with $T_g{}^S$. The β-process occurring between −140 and −150°C for both series of PUs is most clearly seen in the G''/T and tan δ curves [Figs. 3(b) and

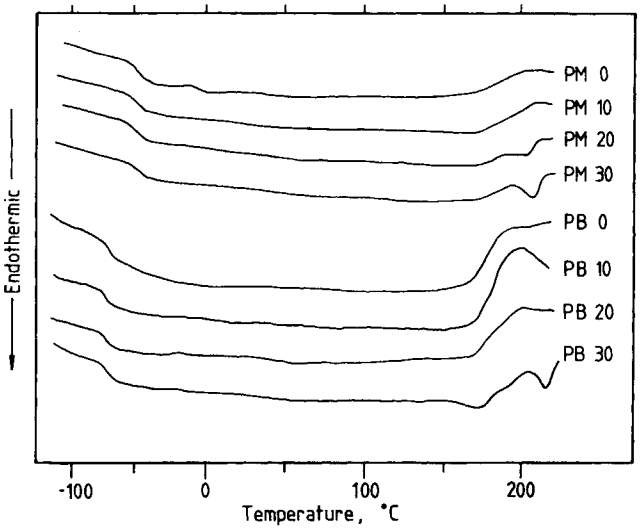

Fig. 1(a). DSC curves from copolyurethanes formed from myrcene- and butadiene-based polyols. Heating rate 20°C min^{-1}; sensitivity 20 mV/cm.

(c)]. It would appear to be due to some secondary motion of the PM and PB chains as it decreases in magnitude on incorporation of hard blocks. The greater magnitude of the process in the PB series relative to the PM series thus suggests that its origins do not lie in side chain motion, because PM chains have a side chain on every repeating unit, irrespective of the mode of propagatioin of polymerization, whereas PB chains have pendent vinylic groups on only ~35% of the repeating units.

The biggest difference between the two series of polymers is observed in the glass transition region. Thus in PM-based copolyurethanes, the tran-

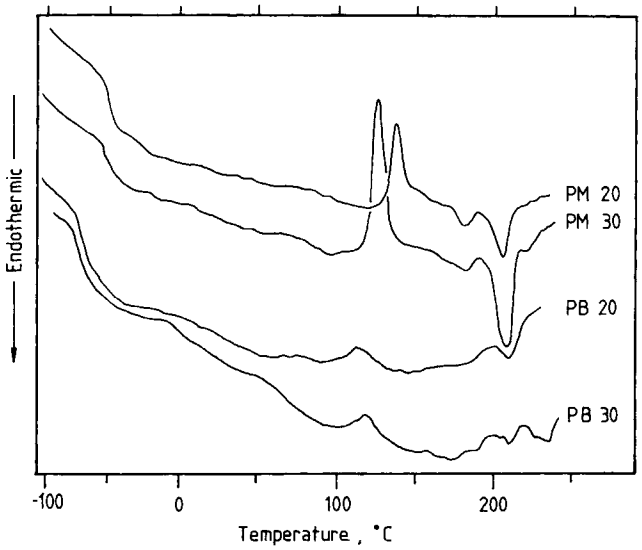

Fig. 1(b). DSC curves from quench-cooled copolyurethanes containing 20 and 30% hard blocks. Heating rate 20°C min^{-1}; sensitivity 5 mV/cm.

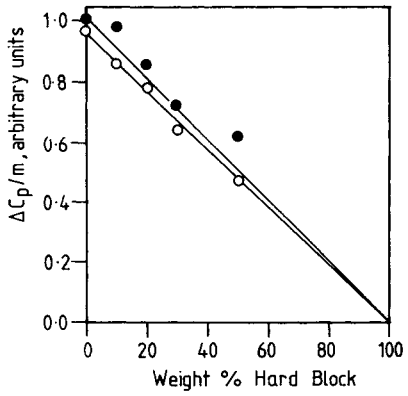

Fig. 2. Degree of phase separation in copolyurethanes formed from myrcene- and butadiene-based polyols: (○) myrcene-based; (●) butadiene-based; (—) behavior expected of phase separation where complete.

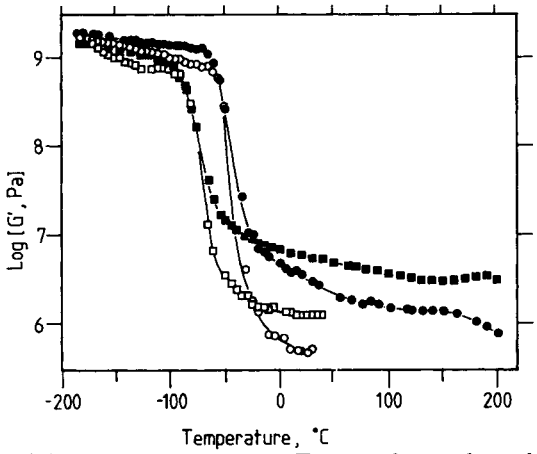

Fig. 3(a). Storage modulus (G') vs. temperature (T) curves for copolyurethanes formed from mycene- and butadiene-based polyols: (○) PM0; (●) PM30; (□) PB0; (■) PB30.

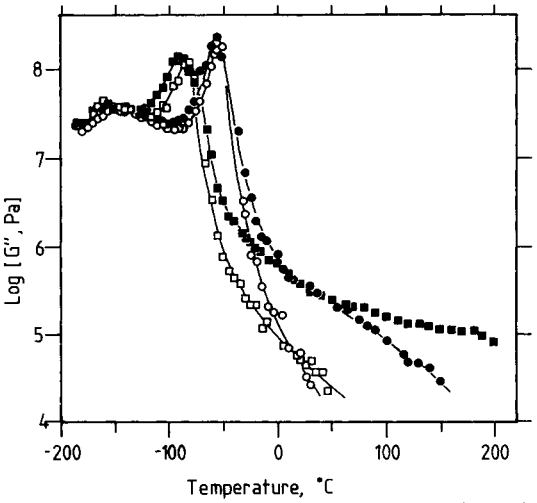

Fig. 3(b). Loss modulus (G'') vs. temperature (T) curves for copolyurethanes formed from myrcene- and butadiene-based polyols: (○) PM0; (●) PM30; (□) PB0; (■) PB30.

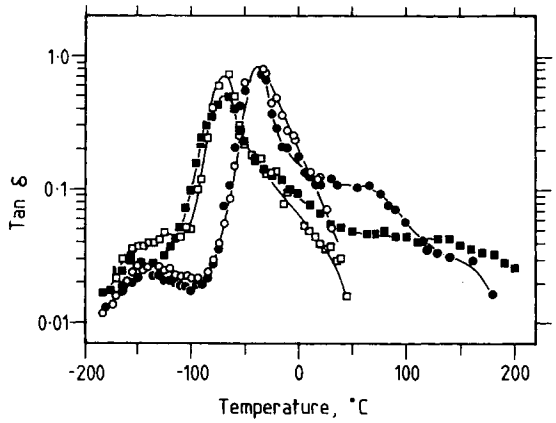

Fig. 3(c). Loss tangent (tan δ) vs. temperature (T) curves for copolyurethanes formed from myrcene- and butadiene-based polyols: (○) PM0; (●) PM30; (□) PB0; (■) PB30.

sition region is ~30°C higher and broader than in the PB series, as also shown by DSC. The values of moduli in the glassy region for the PM-based homopolymer are higher than those of the PB-based homopolymer. The converse is true for the moduli in the rubbery region. The differences in rubbery moduli for PM- and PB-based elastomers may be attributed to differences in sol-fraction contents, to molar mass between crosslinks, $\overline{M}_c$, (in the soft segments), and possibly to the effects of lower functionality of the precursor polyols.

Addition of hard blocks into both PM- and PB-based PUs causes an increase in glassy and rubbery moduli due to constraints and intrinsic stiffness afforded by the crystalline phase. In addition in Figure 3(c) for both series of polymers, the level of damping above T_g increases with increasing hard block content. In PM30 [Fig. 3(c)] there is evidence of a separate damping peak between 50 and 70°C which may be associated with $T_g{}^H$. A much smaller peak at approximately 0°C merging with $T_g{}^S$ is observed for PB30, suggesting that the amount of amorphous material present in the hard block phase is greater in PM30.

The location of $T_g{}^S$ is either series, as indicated by the maximum in the tan δ/T curve, is unaffected by the incorporation of hard blocks, which again correlates with the DSC data discussed earlier.

Swelling and Solubility Behavior

All the PUs studied swelled in toluene without disintegrating or dissolving and thus were crosslinked. The swelling ratios in the PM-based polymers were approximately double those of the corresponding PB-based polymers, again reflecting the differences in $\overline{M}_c$ values for the respective soft segment phases. This observation may be attributed to the differences in functionality evaluated for the two parent polyols (PM and PB), which suggests that the Arco system contains a greater proportion of material having a functionality greater than 2.00 as discussed previously.[11]

The PM-based elastomers had markedly higher sol fractions. The components of the sol fraction could be: (i) zero-functional oligomeric material derived from the thermal Diels–Alder reaction of myrcene described

previously[16]; (ii) zero-functional material resulting from loss of hydroxyl functionality, for example, by dehydration; (iii) zero-functional oligomeric material of idealized structure (C) produced by either MDI or —NCO tipped oligomers reacting with monofunctional hydroxy-containing PM species;

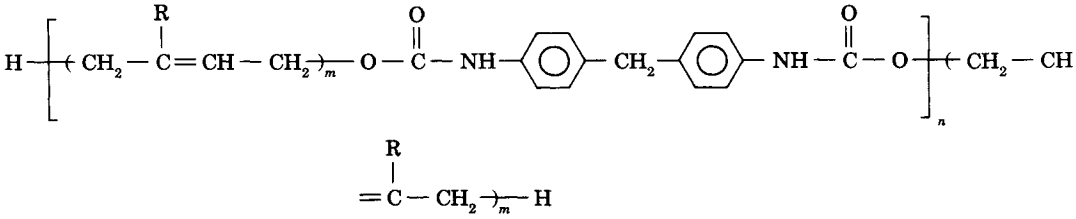

(C) [based on the idealized structure (B)]

(iv) oligomeric species containing unreacted isocyanate groupings; (v) oligomeric species containing unreacted hydroxyl groupings.

In an attempt to establish the nature of the species present in the PM-based sol fractions, they were subjected to GPC and IR analyses. GPC analysis gave the following results: PMO sol fraction: $\overline{M}_n = 3980$; $M_w = 10{,}000$, and $\overline{M}_w/\overline{M}_n = 2.56$; PB sol fraction: $\overline{M}_n = 1890$, $M_w = 4900$ and $\overline{M}_w/\overline{M}_n = 2.67$. In the case of PMO, small peaks were present at the low-molecular-weight end of the chromatogram consistent with species produced by the Diels–Alder reaction.[11]

IR analysis indicated that some of the species present contained urethane groups, but no free hydroxyl or isocyanate groups were detected. The data obtained thus suggest that the sol fraction contains Deils–Alder adducts of myrcene together with urethane containing species whose number-average degree of polymerization does not exceed 2. This implies that these compounds result from the reaction of MDI with monofunctional species having $M_n < 1500$. Thus in structure (C), $m \approx 11$ and $n \not> 2$. These monofunctional species arise from those macroadicals in the polymerizing mixture which undergo termination of polymerization by transfer rather than by combination as illustrated for the idealized, 1,4-propagated sequences of units.

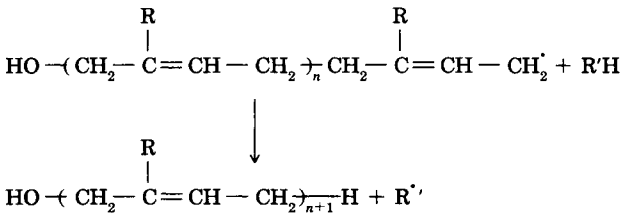

where R=H in PB, R = $-CH_2-CH_2-CH=C\cdot(CH_3)_2$ in PM, and R'H is any species capable of undergoing transfer in the polymerizing medium (solvent, monomer, polymer, or initiator). Myrcene and PM have significantly more allylic hydrogen atoms in their structures than butadiene and PB. This gives rise to more possibilities for transfer and production of monofunctional material, leading to the higher sol fractions observed for PM.

The amount of sol fraction present in both series of copolyurethanes [Fig. 4(a)] decreases as the hard block content increases, reflecting the lower

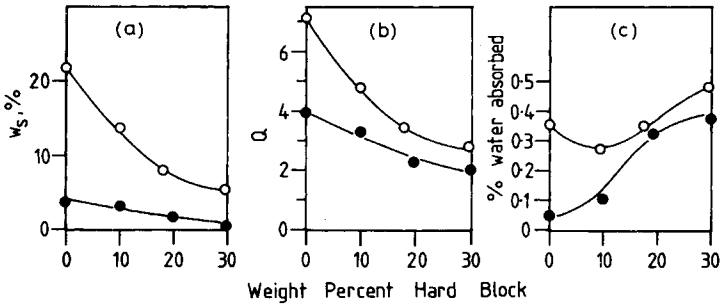

Fig. 4.(a–c). Effect of hard-block content onthe properties of copolyurethanes formed from myrcene- and butadiene-based polyols: (○) myrcene-based; (●) butadiene-based; W_S = sol fraction; Q = swelling ratio in toluene at 20°C.

proportion of liquid rubber present. Swelling ratios [Fig. 4(b)] similarly reflect this trend. The water uptake [Fig. 4(c)] is higher for the PM series but, at all hard-block contents, is less than 0.5% w/w. As the hard-block content increases, the water uptake increases, reflecting the presence of more hydrogen bonding sites within the polymers and possibly an increase accessibility of water to the amorphous phase.

Tensile Stress–Strain Behavior

The tensile stress–strain data for the two series of PUs are plotted in Figures 5(a) and (b) which show behavior typical of elastomeric materials. The tensile properties derived form the curves in Figures 5 are given in Table III, which shows that, in general, these PU elastomers possess lower ultmate properties compared with other common vulcanized rubbers.[18] In both series, the addition of hard blocks tends to improve tensile properties of the respective homopolymers, including an unexpected increase in ultimate elongation at 10% w/w hard block. However, differences between the PM and PB elastomers are apparent and are better illustrated as empirical plots of Young's modulus E, tensile strength σ_u, and ultimate elon-

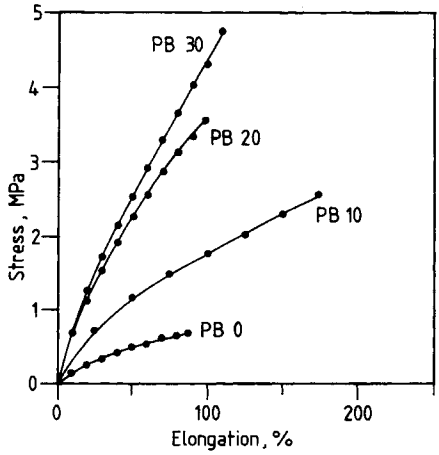

Fig. 5(a). Tensile stress–strain behavior of copolyrethanes formed from butadiene-based polyols.

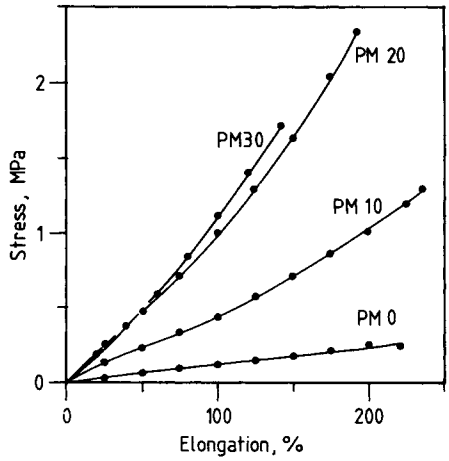

Fig. 5(b). Tensile stress–strain behavior of copolyurethanes formed from myrcene-based polyols.

gation, ϵ_u vs. hard block content as shown in Figure 6. For the PB-based elastomers, E and σ_u increase steadily whereas, for the PM-based elastomers, E reaches a limiting value and σ_u passes through an apparent maximum at 20% w/w hard block content. In terms of ultimate elongation, both series of elastomers show similar trends with a maximum ϵ_u at 10% w/w hard block but with the PM-based elastomers exhibiting significantly higher elongations overall. The general trends in tensile properties of these segmented copolyurethanes are attributed to the pseudocrosslinking and reinforcing effects afforded by the crystalline hard segments. Overall, these observations are in general accord with those of Brunette et al.[19] for copolyurethanes based on Arco, 1,4-butane diol, and toluene diisocyanate.

The PM-based elastomers are intrinsically weaker and softer, and swell to much greater extents than the corresponding PB-based elastomers. These differences may be related, in simplistic terms, to the different values of $\overline{M}_c$, the mean molar mass between crosslinks in these PU networks. Ideally, values of $\overline{M}_c$ can be obtained by analyzing the stress–strain data using the statistical theory of rubber elasticity.[18] In its simplest form, the theory

TABLE III
Tensile Properties of PM and PB-Based PU-Elastomers Containing Various Amounts of Hard Blocks

Polymer code	Young's modulus E (MPa)	Tensile strength σ_u (MPa)	Ultimate elongation ϵ_u (%)
PM0	0.12	0.24	221
PM10	0.56	1.28	235
PM20	1.00	2.33	193
PM30	1.00	1.71	142
PB0	1.35	0.68	87
PB10	3.32	2.57	174
PB20	6.14	3.57	106
PB30	7.04	4.81	113

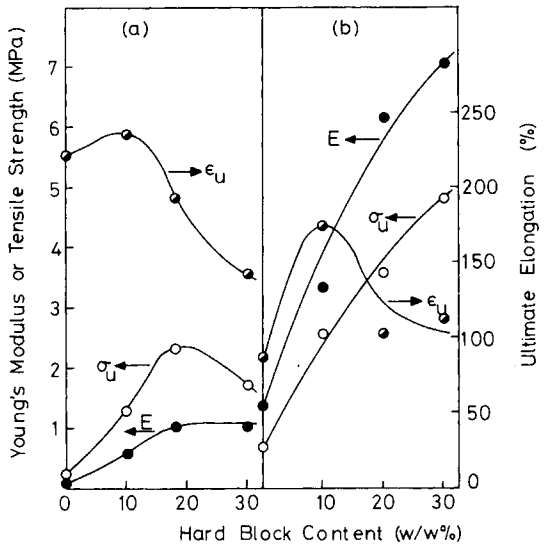

Fig. 6. The effects of hard-block content on the tensile properties of copolyurethane elastomers formed from (a) myrcene- and (b) butadiene-based polyols: (●) Young's modulus (E); (○) tensile strength (σ_u); (○) ultimate elongation (ϵ_u).

predicts that the stress–strain response under equilibrium conditions is given as

$$\sigma = G(\Lambda - \Lambda^{-2}) \tag{1}$$

where σ is the force per unit unstrained area, Λ is the extension ratio, and G is an apparent shear modulus. Plots of σ vs. $(\Lambda - \Lambda^{-2})$ for the PU elastomers given in Table III are shown in Figure 7, where the linearity predicted by eq. (1) is not observed and deviations from linearity increase with hard block content, particularly for the PM series.

In fact, analysis of the copolyurethanes using the statistical theory is not

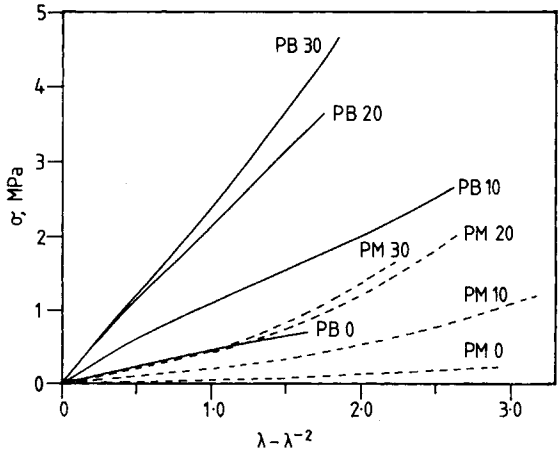

Fig. 7. Stress–strain data plotted according to Gaussian theory[18]: (—) polymyrcene-based PUs; (—) polybutadiene-based PUs.

appropriate due to the extensive energetic interactions[18] between chains which clearly exist. In Figure 7, only in the case of the homopolymers PB0 and PM0 is eq. (1) applicable and even then deviations from linearity are observed. For PM0 the data are essentially linear up to $\Lambda \approx 2.2$ after which value an upward curvature with respect to the abscissa is observable, whereas, for PB0, there is a small but discernible, continuous downward curvature.

Deviations from classical behavior predicted by eq. (1) are most conveniently represented by the semiempirical relation derived by Mooney and Rivlin,[20] namely,

$$\sigma = (\Lambda - \Lambda^{-2})(2C_1 + 2C_2/\Lambda) \tag{2}$$

In eq. (2), $2C_1$ and $2C_2$ are empirical constants independent of Λ and eq. (1), derived from the statistical theory, corresponds to the perticular case $2C_2 = 0$. Tensile data are more usually expressed using the "reduced stress"[21] or modulus σ^*, obtained by rearranging eq. (2), as follows:

$$\sigma^* = \sigma/(\Lambda - \Lambda^{-2}) = (2C_1 + 2C_2/\Lambda) \tag{3}$$

so that a plot of σ^* vs. $1/\Lambda$ should be linear with a slope of $2C_2$ and an intercept on the σ^*-axis of $2C_1$ at $1/\Lambda = 0$, and $(2C_1 + 2C_2)$ at $1/\Lambda = 1$. Thus the value of the modulus is $2C_1$ [equivalent to G in eq. (1)] in the limit at large deformation ($1/\Lambda \rightarrow 0$), and $(2C_1 + 2C_2)$ in the limit at small deformation ($1/\Lambda \rightarrow 1$).

At high deformations ($1/\Lambda = 0$), networks are assumed to exhibit phantom behavior[22] and the modulus $2C_1$ is interpreted using the equation

$$2C_1 = \frac{A_f \rho RT}{\overline{M}_c^{\text{ph}}} \cdot \phi_2^{1/3} \cdot \left(\frac{V_D}{V_F}\right)^{2/3} \tag{4}$$

where for the network ρ is the density, V_F is the volume at formation (reference state), and V_D is the dry volume, after removal of solvent or any sol fraction. For networks tested in the swollen state, ϕ_2 is the volume fraction of newtork, and A_f is the "structure factor" which for an f-functional newtork is given by $1\text{-}2/f$. In the limit of small deformations ($1/\Lambda = 1$) newtorks behave affinely,[21] and the modulus $(2C_1 + 2C_2)$ is interpreted as

$$(2C_1 + 2C_2) = \frac{A \rho RT}{\overline{M}_c^{\text{af}}} \cdot \phi_2^{1/3} \cdot \left(\frac{V_D}{V_F}\right)^{2/3} \tag{5}$$

where the factor A is unity for networks of any functionality.

Plots of σ^* vs. $1/\Lambda$ are shown in Figure 8 for the homopolymers PM0 and PB0 in comparison with earlier data of Gumbrell et al.[23] for vulcanized natural rubber (NR). Plotted in this way, the data for PM0 and PB0 show significant differences in tensile behavior which are further quantified by

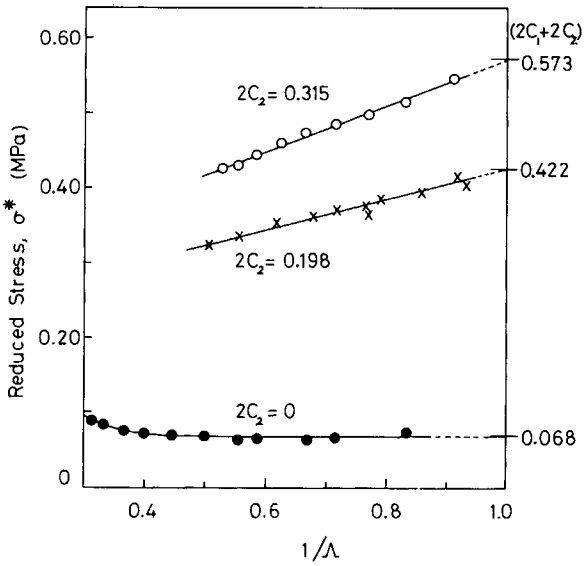

Fig. 8. Mooney–Rivlin plots for homopolyurethane elastomers formed from myrcene- and butadiene-based polyols. Data for vulcanized natural rubber (NR) after Gumbrell et al.[23] is also included: (○) PB0; (●) PM0; (X) NR.

the derived values of $2C_2$ (slopes) and $(2C_1 + 2C_2)$ (low deformation intercepts) shown in Table IV. Deviations from ideality are represented by the value of the elasticity constant $2C_2$, or more generally by the ratio $2C_2/2C_1$, which is really a measure of the extent to which the tensile deformation changes from essentially affine to phantom network with increasing stress. PB0 therefore shows a marked dependence on $1/\Lambda$ and the higher value of $2C_2/2C_1$ compared with NP (1.22, cf. 0.83), structural differences apart, is consistent with the lower functionality (2.68, cf. 4.00) of the former. This observation is also in agreement with data on PDMS networks,[21] which demonstrate that $2C_2/2C_1$ increases with decreasing functionality and is

TABLE IV
Comparative Data for PM- and PB-Based Polyurethane Networks and Vulcanized Natural Rubber[23] Derived from the Mooney–Rivlin Plots in Figure 8

Sample	PM0	PB0	NR
$\underline{M}_n$ (g mol^{-1})[a]	2950	2919	—
f_n	2.23	2.68	4.00
ϕ	0.758	0.992	1.000
$2C_2$ (MPa)	0.000	0.315	0.198
$(2C_1+2C_2)$ (MPa)	0.068	0.573	0.422
$2C_2/2C_1$	0.000	1.221	0.884
$\underline{M}_c^{af}$ (g mol^{-1})[b]	25,605	3934	5692
M_c^{ph} (g mol^{-1})[c]	—	2217	5331
f^2	—	3.64	4.26
n	65	128	251

[a] Determined by GPC, see Table I.
[b] $\underline{M}_c^{af} = \underline{M}_c$ values for affine behavior calculated using eq. (5).
[c] $M_c^{ph} = M_c$ values for phantom behavior calculated using eq. (4).
[d] f = apparent network functionality calculated using eq. (6).

directly related to the looseness with which the crosslinks are embedded in the network structure. On the other hand, PM0 shows almost ideal behavior up to $1/\Lambda = 0.4$ with $2C_2/2C_1 = 0$, and the difference in behavior compared with PB0 must be attributed principally to the presence of a large amount of sol fraction as indicated by the values of ϕ_2 in Table IV. Swelling has long been known to decrease $2C_2/2C_1$ very markedly, [23] and $2C_2/2C_1$ has been shown to decrease to zero with increasing swelling representing a systematic reduction and ultimate disappearance of the deviations from ideal behavior.

Values of $\overline{M}_c^{af}$ and $\overline{M}_c^{ph}$, shown in Table IV, have been calculated using eq. (4) and (5), respectively, except for PM0 for which $2C_2 = 0$ and eq. (5) only is applicable. The $\overline{M}_c$ values for PB0 are clearly different, which is physically or structurally inconsistent, and, accepting the imperfect nature of these PU networks, this difference is because either the large deformation limit is not truly phantom or that the value of $\overline{f}_n$ used in eq. (4) to calculate $\overline{M}_c^{ph}$ is uncertain. Furthermore, if the assumption that the deformation of a network can undergo transition from perfectly affine to perfectly phantom as $1/\Lambda$ decreases from unity to zero is valid, then the combination of eq. (4) and (5) gives

$$\frac{2C_2}{(2C_1+2C_2)} = (1-A_f) = \frac{2}{f} \tag{6}$$

The ratio $2C_2/(2C_1+2C_2)$ can be evaluated form the data of Figure 8 as the ratio of slope $(2C_2)$ to low deformation intercept $(2C_2+2C_1)$. Using eq. (6), the value of f obtained for PB0 is 3.64, which is significantly and unaccountably higher than that for $\overline{f}_n$ (=2.68). Accepting that the linear data of Figure 8 must be self-consistent (and considering also the values of f and $\overline{M}_c$ for NR), the disparity is probably due to the inapplicability of phantom behavior at large deformations to these particular PU networks.

Comparing then the values of $\overline{M}_c^{af}$ (25,605, cf. 3,934) for PM0 and PB0 in relation to their respective $\overline{M}_n$ values 2950, cf. 2919) it must be concluded that PM0 comprises a much broader distribution of chain lengths and a larger proportion of dangling chains in the network. This conclusion is substantiated in part by the sol fraction analysis of PM0 and the low value of $\overline{f}_n$ in Table I, both of which indicate the presence of substantial amounts of mono- and bifunctional hydroxy oligomers together with higher functional hydroxymaterial in the original polymyrcene polyol.

An interesting feature in Figure 8 observed only for PM0, as an anomalous, gradual upturn in σ^* with increasing elongation commencing at a $1/\Lambda$ value of 0.4. Such behavior may be expected to arise from two sources. First, there is the possibility of strain-induced crystallinity, but this is unlikely in the polymyrcene-based network, bearing in mind the bulkiness of the substituent $-C_6H_{11}$ attached to each myrcene unit [see the idealized soft segment unit (B)]. Second, the upturn is probably attributable to finite chain extensibility associated with the shorter network chains containing only small numbers, $\overline{n}$, of skeletal bonds. Mean values of $\overline{n}$, 65 and 128 in Table IV, for the shortest chains in PM0 and PB0 networks respectively can be calculated form the $\overline{M}_n$ and $\overline{f}_n$ data in Table I, assuming ideal

network formation based on the idealized structures (B) of the respective soft segment units. The much smaller value for $\bar{n}$ for PM0 therefore takes account of the molar mass of the $-C_6H_{11}$ substituent and is typical of the $\bar{n}$ values determined for short chains used in bimodal PDMS networks[21] for which similar upturns in Mooney–Rivlin plots were also observed.

CONCLUSIONS

Polyols derived from mycrene are clearly capable of being used to form elastomeric PUs whose properties are similar to those based on commercially available polyols derived from butadiene. The physical properties of homopolyurethanes based on polymyrcene (PM) and polybutadiene (PB) polyols are generally inferior to conventional crosslinked rubbers. However, marked improvements in properties were achieved by the incorporation of crystalline hard blocks, based on 1,4-butane diol, which, during copolyurethane preparation, phase-separated almost completely from the soft-block phase (the sole component of the homopolyurethanes).

The differences in physical properties were shown to be governed by the chemical and microstructural features of the PM and PB polyols, the distribution of molecular species present and their functionalities ($\bar{f}_n$) towards MDI. The lower $\bar{f}_n$ value (2.23) for PM compared with that for PB (2.68) was shown to produce a significantly greater, residual sol fraction in the crosslinked PUs formed from the PM polyol. For the latter, analysis of the sol fraction showed the existence of low molar mass material comprising zero-functional species present in the original PM and urethane-containing oligomers formed from monofunctional PM species during elastomer formation.

Thermal analyses (DSC and DMA) thus showed differences in T_g between the PM- and PB-based PU elastomers, with values in the range −40 to −60°C and −70 to −80°C, respectively, independent of hard block content. T_g differences clearly influence the elastomeric behavior at ambient temperature, as shown by the stress–strain data. Analysis of the stress–strain data for the homopolyurethanes showed that both PM and PB systems can be desceibed by the Mooney–Rivlin expression to yield values of $(2C_1 + 2C_2)$ (shear moduli) and $2C_2/2C_1$ (deviations from ideal behavior). In these terms, the PM elastomer which was effectively swollen by its significant sol fraction had a modulus of $(2C_1 + 2C_2) = 0.068$ MPa and showed almost ideal behavior ($2C_2/2C_1 = 0$) up to at least 150% strain, at which point finite chain extensibility became important. The PB elastomers with a modulus of $(2C_1 + 2C_2) = 0.573$ MPa, however, showed deviations from ideal behavior ($2C_2/2C_1 = 1.221$) and the assumption of phantom chain behavior at high strains was shown to be invalid. Interpretation of $(2C_1 + 2C_2)$ using Gaussian theory, which accounts for functionality and sol fraction differences, produced vastly different $\bar{M}_c$ values, 25,605 and 3,934 g mol^{-1}, respectively, for PM- and PB-based elastomers.

Finally, this study has shown that a range of PU materials, which can be formed by a simple casting process, have useful properties typical of other elastomers. These materials can be produced from an abundant, naturaly derivable terpene which is obtained as a byproduct of the paper-pulping industry.

References

1. D. C. Sayles, *Rubber Chem. Technol.*, **39**, 112 (1966).
2. United Technology Corp, U. S. Pat. 4,263,071 (1974).
3. Takeda Chemical Industries Ltd. and Ipposha Oil Industries Ltd., Jpn. Pat. 8182864 (1981).
4. F. Wilson, U. S. Pat. 4,063,022 (1975).
5. K. Nate, Jpn. Pat. 777,140 (1977).
6. B. B. Idate, S. P. Vernekar and N. D. Ghatge, *J. Polym. Sci., Polym. Chem. Ed.*, **21**, 385 (1983).
7. C. Pinazzi, G. Legeay and J.-C. Brosse, *Makromol. Chem.*, **176**, 2509 (1975).
8. D. N. Schulz, A. F. Halasa, and A. E. Oberster, *J. Polym. Sci., A1*, **12**, 153 (1974).
9. C. Hepburn, Ed., *Polyurethane Elastomers*, Applied Science, London, 1982.
10. Y. J. P. Chang and G. L. Wilkes, *J. Polym. Sci., Polym. Phys. Ed.*, **13**, 455 (1975).
11. J. L. Cawse, J. L. Stanford, and R. H. Still, *J. Appl. Polym. Sci.*, to appear.
12. C. M. Brunette, S. L. Hsu, W. J. MacKnight, and N. S. Schneider, *Polym. Eng. Sci.*, **21**, 163 (1981).
13. H. E. Stagg, *The Analyst*, **71**, 557 (1946).
14. N. S. Schneider and R. W. Matton, *Polym. Eng. Sci.*, **19**, 1122 (1979).
15. P. W. Ryan, *Br. Polym. J.* **3**, 145 (1971).
16. J. L. Cawse, J. L. Stanford, and R. H. Still, *Makromol. Chem.* **185**, 709 (1984), Part II of this series.
17. J. Blackwell, M. R. Nagarajan, and T. B. Haitink, *Polymer*, **23**, 951 (1982).
18. L. R. G. Treloar, *The Physics of Rubber Elasticity*, 3rd ed., Oxford Univ. Press, Oxford, 1975.
19. C. M. Brunette, S. L. Hsu, M. Rossman, W. J. MacKnight, and N. S. Schneider, *Polym. Eng. Sci.*, **21**, 668 (1981).
20. (a) M. Mooney, *J. Appl. Phys.*, **19**, 434 (1948); (b) R. S. Rivlin, *Phil. Trans. Roy. Soc. London*, **A241**, 379 (1948).
21. J. E. Mark, *Adv. Polym. Sci.*, **44**, 1 (1982).
22. P. J. Flory, *Proc. Roy. Soc. London*, **A351**, 351 (1976).
23. S. M. Gumbrell, L. Mullins, and R. S. Rivlin, *Trans. Faraday Soc.*, **49** 1495 (1953).

Received April 1, 1985
Accepted September 20, 1985